CrossMark

ORIGINAL PAPER

Methanol Steam Reforming on Perovskite-Type Oxides $LaCo_{1-x-y}Pd_xZn_yO_{3\pm\delta}$: Effect of Pd/Zn on CO_2 Selectivity

Jagoda Kuc[1] · Anke Weidenkaff[1,2] · Santhosh Kumar Matam[1]

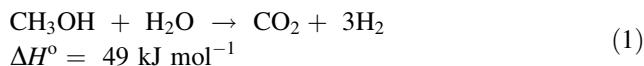**Abstract** The perovskite-type oxides $LaCoO_{3\pm\delta}$ (LCO) with and without substitution of Co by Pd and/or Zn are studied for steam reforming of methanol (SRM). The catalysts $LaCo_{1-x-y}Pd_xZn_yO_{3\pm\delta}$ are synthesized by amorphous citrate method and subjected to calcination at 800 °C for 2 h. The catalysts are characterized by inductively coupled plasma optical emission spectroscopy (ICP-OES), N_2-physisorption (BET), X-ray diffraction (XRD) and tested in SRM reaction. The surface area of the catalysts is around 9 ($\pm$1) m²/g. The XRD patterns of the catalysts reflect only rhombohedral crystal structure, indicating the phase purity of the perovskites. The SRM performance of the catalysts, especially the CO_2 selectivity below 275 °C, is strongly dependent on the catalyst composition and reaction temperature. The CO_2 selectivity profile of Pd and Zn containing $LaCo_{0.85}Pd_{0.075}Zn_{0.075}O_{3\pm\delta}$ consists of two distinct maxima, one at 225 °C and the other above 375 °C. The former is missing on un-substituted LCO or mono metal substituted $LaCo_{0.87}Pd_{0.13}O_{3\pm\delta}$ and $LaCo_{0.89}Zn_{0.11}O_{3\pm\delta}$, which is attributed to CO_2 selective phase related to Pd and Zn. The high temperature CO_2 selectivity maximum of the catalysts is not dependent on the Co substitution by Pd and/or Zn and is ascribed, in general, to the bulk catalyst composition.

Keywords $LaCoO_{3\pm\delta}$ · $LaCo_{1-x-y}Pd_xZn_yO_{3\pm\delta}$ · SRM · CO_2 selectivity

✉ Santhosh Kumar Matam
    santhosh.matam@empa.ch

[1] Empa, Swiss Federal Laboratories for Materials Science and Technology, 8600 Dübendorf, Switzerland

[2] Materials Chemistry, Institute for Materials Science, University of Stuttgart, 70569 Stuttgart, Germany

1 Introduction

Perovskite-type oxides have received a great deal of attention in the recent past due to their interesting physical and chemical properties which make them potential candidates for a wide range of applications such as in catalysis [1–3], electro-catalysis [4], photo-catalysis [5] and thermoelectricity [6]. The general chemical formula of a perovskite-type oxide is $ABO_{3\pm\delta}$; where A represents rare earths (e.g., La) or alkali/alkaline earth (e.g., Ca) metal cations, while B depicts transition metal cations (such as Co). Metal cation A is larger than B cation and is in a 12-fold coordination, while B cation is in a six fold coordination [1, 2] as shown in Fig. 1. The physical and chemical properties of the materials can be tailor made for specific applications by partial substitution of A and/or B site cations with other suitable elements, whilst preserving the perovskite crystal structure [1–7]. These metal cations are in close interactions due to the covalent nature of the bonds in the compounds which exhibit remarkable catalytic properties, for example $LaFe_{0.57}Co_{0.38}Pd_{0.05}O_3$ as three-way catalysts [8]. The flexibility of crystal structure to accommodate multiple A and/or B site cations in a single composition is a promising approach for developing the steam reforming of methanol (SRM) catalysts. Based on this concept, we report perovskite-type oxide $LaCoO_{3\pm\delta}$ with and without Co substitution by Pd and/or Zn ($LaCo_{1-x-y}Pd_xZn_yO_{3\pm\delta}$) for SRM reaction (Eq. 1).

$$CH_3OH + H_2O \rightarrow CO_2 + 3H_2$$
$$\Delta H^o = 49 \text{ kJ mol}^{-1} \tag{1}$$

The undesired CH_3OH decomposition (Eq. 2) and reverse water gas shift reaction (RWGS) (Eq. 3) occur simultaneously to SRM [9, 10].

Fig. 1 $ABO_{3\pm\delta}$ perovskite-type oxide structure

$$CH_3OH \rightarrow CO + 2H_2 \qquad \Delta H^o = 91 \text{ kJ mol}^{-1} \qquad (2)$$

$$CO_2 + H_2 \rightarrow CO + H_2O \qquad \Delta H^o = 41.2 \text{ kJ mol}^{-1} \qquad (3)$$
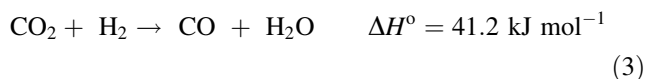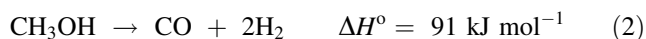
These two undesired side reactions can be thermodynamically limited by conducting SRM at lower temperatures with suitable catalysts. A few studies report perovskite-type oxides such as $La_{0.6}Sr_{0.4}Co_{1-y}Fe_yO_{3-\delta}$ (y = 0.2, 0.5, 0.8) [11], $LaCo_{0.7}Cu_{0.3}O_3$ [12] and $La_{0.7}Sr_{0.3}CuO_{3-\delta}$ [13] for SRM reaction for solid oxide fuel cell (SOFCs) applications. The SRM performance of these catalysts is, in general, very poor; CH_3OH conversion activity of the catalysts begins only above 250 °C and the CO_2 selectivity is between 50 and 70 %. For example, the CO_2 selectivity of $La_{0.6}Sr_{0.4}Co_{1-y}Fe_yO_{3-\delta}$ (y = 0.2, 0.5, 0.8) is around 50 % indicating the simultaneous occurrence of SRM and CH_3OH decomposition over the catalysts [11]. Besides decomposition reaction, methanation is also reported. Against this background, $LaCo_{1-x-y}Pd_xZn_yO_{3\pm\delta}$ is studied aiming to improve the overall low temperature (<250 °C) SRM performance of the catalysts, especially CO_2 selectivity. The results suggest that the CO_2 selectivity of the catalysts is sensitive to $LaCo_{1-x-y}Pd_xZn_yO_{3\pm\delta}$ composition.

2 Experimental

2.1 Catalyst Preparation

The perovskite-type oxide $LaCoO_{3\pm\delta}$ was synthesized with and without Co partial substitution by Pd and/or Zn ($LaCo_{1-x-y}Pd_xZn_yO_{3\pm\delta}$) by the amorphous citrate method. Metal precursors [$La(NO_3)_3\cdot6H_2O$ (Alfa Aesar, 99,9 %),

$Co(NO_3)_3\cdot6H_2O$ (Alfa Aesar), $Zn(NO_3)_3\cdot6H_2O$ (Alfa Aesar, 99.9 %) and $Pd(NO_3)_3$ solution (Alfa Aesar 4.42 % w/w Pd cont.)] and citric acid monohydrate (Alfa Aesar, 99 %) were utilized. The detailed synthesis procedure was described elsewhere [14]. Briefly, desired amounts of metal precursors were dissolved in deionized water and subsequently citric acid was added in a metal to acid molar ratio of 1:1. The solution was evaporated in a rotary evaporator at 70 °C to obtain a viscous solution, which was then dried overnight at 80 °C in a vacuum oven and was subjected to calcination in air at 800 °C for 2 h. For the sake of clarity, the catalyst compositions are abbreviated as shown in Table 1.

2.2 Characterization

2.2.1 Inductively Coupled Plasma Optical Emission Spectrometry (ICP-OES)

The chemical composition of the perovskite-type oxide catalysts was determined by ICP-OES analyzer (Vista RL, Varian). For each experiment, around 10 mg of catalyst powder was dissolved in aqua regia using an ultrasonic bath and subsequently analyzed.

2.2.2 N_2 Physisorption

The total surface area of the catalysts was determined by the Brunauer–Emmett–Teller (BET) method [15] using nitrogen adsorption and desorption isotherms that were obtained at −196 °C on a Micromeritics ASAP 2020c instrument.

2.2.3 X-ray Diffraction (XRD)

The powder XRD patterns of the catalysts were obtained on a PANalytical X'Pert PRO θ–2θ scan system using Cu $K\alpha_1$ radiation (1.5406 Å, 45 kV and 40 mA).

2.3 Steam Reforming of Methanol (SRM)

The SRM experiments were carried out at atmospheric pressure using a plug flow quartz reactor (d_i = 6 mm and l = 400 mm) equipped with gas manifold (Bronkhorst) and gas analyzing systems (GC and MS). The reactor was loaded with catalyst particles (100 mg and sieve fraction of 150–200 μm) that were mixed with quartz particles of the same size and firmly packed between two plugs of quartz wool. The catalyst bed temperature was measured with a K-type thermocouple. Prior to the SRM reaction, the catalysts were pre-treated in air at 500 °C for 1 h and then cooled to 100 °C. At this temperature, the SRM reaction mixture of H_2O and CH_3OH (1.3:1 volume ratio) in He was fed to the reactor at a total flow rate of 100 ml/min. The

Table 1 Chemical composition and physical and SRM properties of the catalysts

Catalyst	Chemical composition[a]	Metal (wt%)		BET (m^2/g)	SRM performance at 225 °C		
		Pd	Zn		CH_3OH con. (%)	CO_2 sel. (%)	H_2 rate (mmol/g_{cat}/h)[b]
LCO	$LaCoO_{3\pm\delta}$	–	–	9	0	0	0
LCPO	$LaCo_{0.87}Pd_{0.13}O_{3\pm\delta}$	5.3	–	10.5	66	8	58
LCZO	$LaCo_{0.89}Zn_{0.11}O_{3\pm\delta}$	–	2.9	10.5	0.5	9.5	4.5
LCPZO	$LaCo_{0.85}Pd_{0.075}Zn_{0.075}O_{3\pm\delta}$	3.2	2.0	7.5	4.5	45	10

[a] Determined by ICP-OES analysis

[b] Based on inlet flow rate

reaction products were analyzed at the reactor outlet by gas chromatograph (3000A microGC, Agilent Technologies equipped with PoraPLOT Q and Molecular Sieve 5A columns) and mass spectrometer (Pfeiffer Omni, 1–200 amu).

# 3 Results and Discussion

3.1 Characterization

The composition and the surface area (S_{BET}) of the catalysts are presented in Table 1. The ICP-OES data confirm the nominal Pd and Zn content in the catalysts, indicating the efficiency of the synthesis method. The S_{BET} of the un-substituted LCO is 9 m^2/g which increases slightly (10.5 m^2/g) upon substitution of Co with either Pd or Zn. This is in line with the literature that reports that the partial substitution of Co by Pd decreases the crystallite size of the perovskite $LaCo_{0.95}Pd_{0.05}O_3$ and hence increases the specific surface area [16]. However, substitution of Co with both Pd and Zn slightly decreases the S_{BET} to around 7.5 ($\pm$1) m^2/g.

The XRD patterns of the catalysts are shown in Fig. 2. It can be readily seen that the un-substituted LCO as well as Pd and/or Zn substituted $LaCo_{1-x-y}Pd_xZn_yO_{3\pm\delta}$ exhibit identical XRD reflections which can be attributed to

Fig. 2 XRD patterns of the catalysts

rhombohedral perovskite crystal structure with the $R\bar{3}c$ space group (PDF card number 01-084-0848) [17, 18]. No other reflections assignable to secondary phases are detected, indicating the phase purity of the perovskites. The XRD reflections of substituted perovskite-type oxides $LaCo_{1-x-y}Pd_xZn_yO_{3\pm\delta}$ are located at slightly lower 2θ angles as compared to that of LCO. The slight shift in the 2θ angles indicates the unit cell expansion of the perovskite crystal due to the substitution of Co cations with Pd and/or Zn of larger ionic radii [19]. These results show that the perovskite-type oxide structure of $LaCoO_{3\pm\delta}$ is preserved with partial substitution of Co cations by Pd and/or Zn ions in $LaCo_{1-x-y}Pd_xZn_yO_{3\pm\delta}$, in line with our previous observations [18]. The single phase rhombohedral crystal structure and comparable surface area (9 ($\pm$1) m^2/g) of the catalysts suggest the similar physical and textural properties among the catalysts.

3.2 Steam Reforming of Methanol (SRM)

The temperature dependent CH_3OH conversion and CO_2 selectivity profiles of the catalysts are shown in Fig. 3. The SRM performance of the catalysts is strongly dependent on the catalyst composition. The un-substituted LCO shows detectable CH_3OH conversion only at around 350 °C and complete conversion is observed at around 500 °C. The activity of the catalyst significantly improves after substitution of Co with Pd and/or Zn. Among the catalysts, Pd containing LCPO exhibits the best CH_3OH conversion activity followed by bimetallic LCPZO and monometallic Zn containing LCZO. On LCPO, conversion begins at 100 °C and completes at 260 °C. The improved SRM activity of the LCPO, as compared to LCO, is attributed to Pd that mainly promotes CH_3OH decomposition reaction (Eq. 2) as reported in [10, 23]. This is in agreement with previous reports that the oxidation activity of LCO significantly improves upon substitution of Co with Pd [18]. This is further corroborated by the SRM activity of LCZO, without Pd (see Fig. 2). The LCZO activity, which begins at 220 °C and ends at 430 °C, is better than the un-substituted LCO but much lower than that of LCPO. These
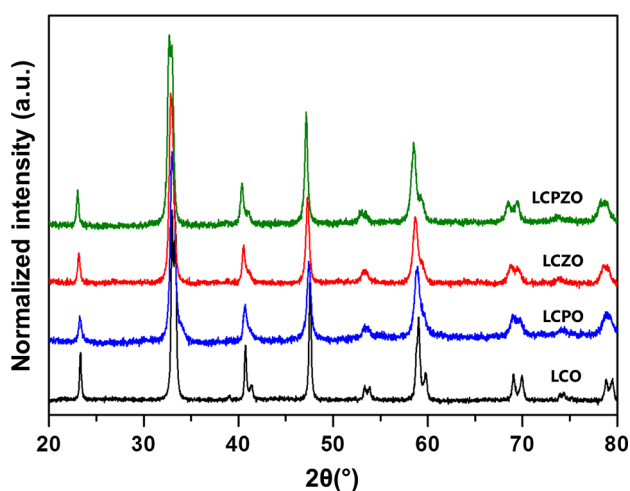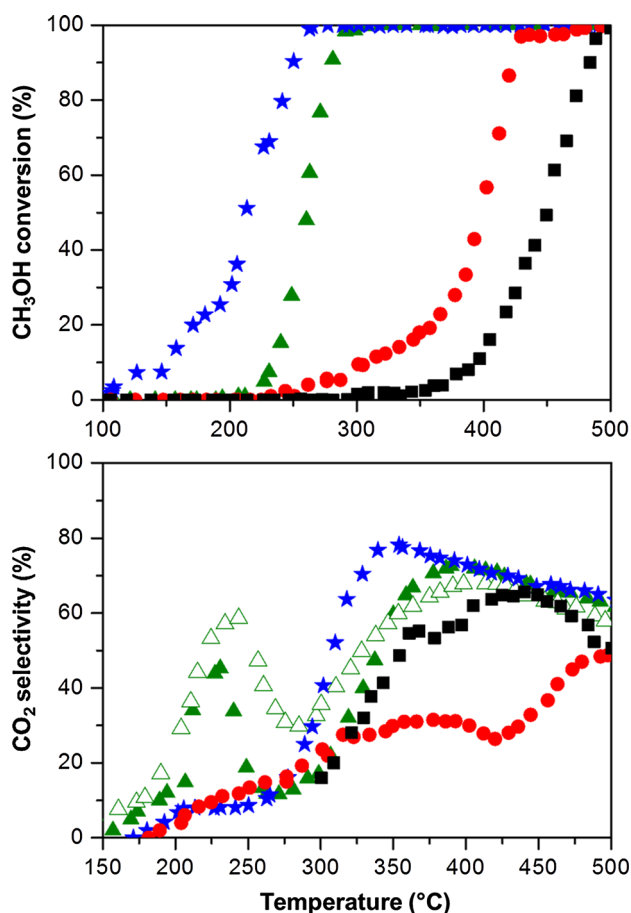
Fig. 3 The SRM activity of the catalysts: LCO (*squares*), LCZO (*circles*), LCPO (*stars*) and LCPZO (*triangles*). *Open triangles* profile is obtained after reductive pre-treatment, please refer text for details. See Sect. 2.3 for reaction conditions

results indicate that Pd is more active for CH_3OH conversion but less selective for CO_2 than Zn, which is again in line with previous reports [9, 10, 20–22]. In agreement with this, the bimetallic LCPZO shows moderate activity that falls between the LCPO and LCZO with conversion starting at 200 °C and completing at around 290 °C.

The CO_2 selectivity of the catalysts is strongly dependent on the catalyst composition, especially below 275 °C. The CO_2 selectivity of the un-substituted LCO is not comparable to the other catalysts below 300 °C due to the negligible CH_3OH conversion. Above this temperature, CO_2 selectivity steadily increases with temperature up to 450 °C followed by a slight decrease. Despite significant difference in the CH_3OH conversion activity of LCPO and LCZO, the CO_2 selectivity of the catalysts is comparable (9 %) at 225 °C. Above 300 °C, the CO_2 selectivity of the catalysts is significantly different. In a marked contrast, the CO_2 selectivity profile of the bimetallic catalyst LCPZO consists of two distinct maxima. The low temperature maximum (of 45 %) is centered at 225 °C, which is not present either on the un-substituted LCO or monometal Pd

or Zn substituted LCPO and LCZO. This indicates the important role of Pd and Zn in CO_2 selectivity. The high temperature CO_2 selectivity maximum (of around 70 %) is above 375 °C on LCPO and LCPZO. It should be mentioned that LCPO shows slightly better CO_2 selectivity between 300 and 375 °C with a maximum of 80 % (with 100 % conversion) at 375 °C. This is the best selectivity reported so far on any $ABO_{3\pm\delta}$ type perovskite oxide [11–13]. The temperature dependent CO_2 selectivity is also evaluated at constant CH_3OH conversion over the catalysts between 150 and 450 °C [24]. These results confirm that the low temperature CO_2 selectivity is govern by the catalyst composition while at high temperatures RWGS (Eq. 3) diminishes the selectivity. The occurrence of the latter indicates an important role of thermodynamics in SRM reaction over these catalysts. The peculiar CO_2 selectivity profile comprising of two distinct maxima on LCPZO is not observed on previously reported perovskite-type oxide catalysts [11–13] and is tentatively assigned to the dynamic behaviour of the active/selective phase composition in the catalyst as a function of temperature during the SRM reaction [14].

The SRM performance of the catalysts is further analyzed at 225 °C and is compared in Fig. 4. At this temperature, LCO does not show any activity. By partial substitution of Co with Zn, the activity (expressed in H_2 formation rate; mmol H_2/g_{cat}/h) improves considerably for LCZO. Whereas, the activity significantly increases for Pd substituted LCPO. The H_2 formation rate is 4.5 and 58 times higher on LCZO and LCPZO, respectively, than on the un-substituted LCO. However, the CO_2 selectivity on LCZO and LCPO is comparable (c.a., 9 %). Based on this, the main contribution to the high H_2 formation rate on LCPO is attributed to the CH_3OH decomposition reaction
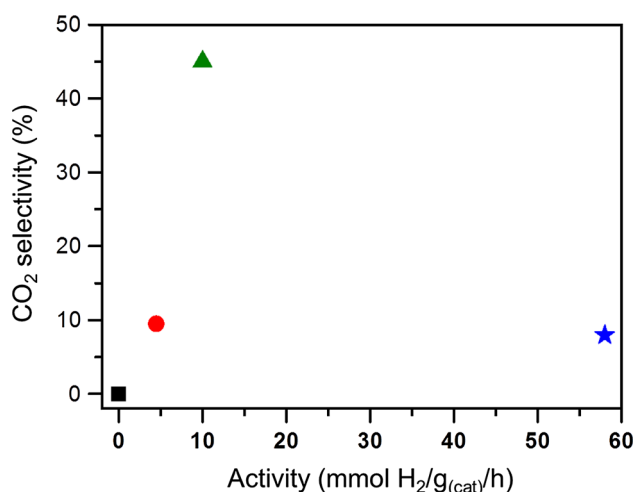

Fig. 4 The SRM activity of the catalysts at 225 °C: LCO (*square*), LCZO (*circle*), LCPO (*star*) and LCPZO (*triangle*). Refer Sect. 2.3 for reaction conditions

(Eq. 2) that occurs on Pd [10, 23]. By substitution of Co with both Pd and Zn, not only H_2 formation rate but also CO_2 selectivity improves on LCPZO (Fig. 4). These results are in agreement with previous studies on supported Pd catalysts for SRM. The CO_2 selectivity of supported Pd catalysts is strongly dependent on the support. Pd supported on SiO_2 and Al_2O_3 mainly catalyses CH_3OH decomposition reaction (Eq. 2) giving rise to merely CO and H_2 [23]. This is dramatically altered for the Pd supported on ZnO catalyst that performs selectively the SRM reaction (Eq. 1). The selective SRM performance of Pd/ZnO catalyst is attributed to PdZn alloy. In agreement with this, the CO_2 selectivity of the catalyst further increases on reductive pre-treatment above 300 °C that promotes PdZn alloy formation [23]. Likewise, supported ZnPd intermetallic nanoparticles are produced by reductive pretreatment of ternary Hydrotalcite-like compounds (comprising of Pd and Zn) to derive SRM catalysts. Such a catalyst exhibits 60 % CO_2 selectivity with 14 % CH_3OH conversion at 250 °C under the studied conditions [25]. Based on these results, the effect of reductive pretreatment on the CO_2 selectivity of LCPZO is studied. To this end, LCPZO is subjected to reductive pre-treatment at 600 °C for 1 h followed by SRM reaction (see open triangles in Fig. 3). The reductive pretreatment improves significantly the low temperature CO_2 selectivity (from c.a., 45–60 %) of the catalyst LCPZO, in excellent agreement with the literature. However, the CH_3OH conversion is comparable for the catalyst LCPZO with (not shown) and without reductive pretreatment. The improved low temperature CO_2 selectivity is attributed to the ZnPd nanoparticles that might have formed upon reductive pretreatment as concluded previously [9, 21–26]. The high temperature CO_2 selectivity of the reductively pretreated LCPZO is comparable with other catalysts (except LCZO) (Fig. 3). These results demonstrate that the low temperature SRM performance of the un-substituted LCO is very poor, which can be greatly improved by partial substitution of Co with Pd and Zn and by reductive pre-treatment. Therefore, further studies are in progress aiming to improve the low temperature CO_2 selectivity further by varying Pd/Zn content in LCPZO, reductive-pretreatment temperature and feed composition [14].

4 Conclusions

The perovskite-type oxides $LaCoO_{3\pm\delta}$ (LCO) with and without partial substitution of Co by Pd and/or Zn are synthesized by amorphous citrate method and tested for steam reforming of methanol (SRM). The characterization results indicate that the physical and textural properties of the catalysts are similar. The SRM performance of the catalysts is strongly dependent on the composition and reaction temperature. The improved low temperature (around 225 °C) CO_2 selectivity of $LaCo_{0.85}Pd_{0.075}Zn_{0.075}O_{3\pm\delta}$ (LCPZO) is attributed to Pd and Zn species as evident from the poor low temperature CO_2 selectivity of LCO and $LaCo_{0.87}Pd_{0.13}O_{3\pm\delta}$ (LCPO) or $LaCo_{0.89}Zn_{0.11}O_{3\pm\delta}$ (LCZO) that do not contain Pd and Zn. However, the CO_2 selectivity above 375 °C is similar for the catalysts, which is in general ascribed to the bulk catalyst composition.

References

1. Seiyama T (1992) Catal Rev Sci Eng 34:281
2. Peña MA, Fierro JLG (2001) Chem Rev 101:1981
3. Matam SK, Eyssler A, Hug P, van Vegten N, Baiker A, Weidenkaff A, Ferri D (2010) Appl Catal B 94:77
4. Adler SB (2004) Chem Rev 104:4791
5. Maegli AE, Hisatomi T, Otal EH, Yoon S, Pokrant S, Gratzel M, Weidenkaff A (2012) J Mater Chem 22:17906
6. Robert R, Aguirre MH, Bocher L, Trottmann M, Heiroth S, Lippert T, Döbeli M, Weidenkaff A (2008) Solid State Sci 10:502
7. Mishra A, Prasad R (2014) Catal Rev Sci Eng 56:57
8. Nishihata Y, Mizuki J, Akao T, Tanaka H, Uenishi M, Kimura M, Okamoto T, Hamada N (2002) Nature 418:164
9. Armbrüster M, Behrens M, Föttinger K, Friedrich M, Gaudry É, Matam SK, Sharma HR (2013) Catal Rev Sci Eng 55:289
10. Iwasa N, Kudo S, Takahashi H, Masuda S, Takezawa N (1993) Catal Lett 19:211
11. Natile MM, Poletto F, Galenda A, Glisenti A, Montini T, Rogatis LD, Fornasiero P (2008) Chem Mater 20:2314
12. Glisenti A, Galenda A, Natile MM (2013) Appl Catal A 453:102
13. Glisenti A, Galenda A, Natile MM (2013) Catal Lett 143:254
14. Kuc J, Neumann M, Armbrüster M, Yoon S, Weidenkaff A, Matam SK (2014 submitted)
15. Brunauer S, Emmett PH, Teller E (1938) J Am Chem Soc 60:309
16. Sartipi S, Khodadadi AA, Mortazavi Y (2008) Appl Catal B 83:214
17. Glosset NMLNP, Van Doorn RHE, Kruidhof H, Boeijsma J (1996) Powder Diffr 11:31
18. Eyssler A, Winkler A, Safonova O, Nachtegaal M, Matam SK, Hug P, Weidenkaff A, Ferri D (2012) Chem Mater 24:1864
19. Shannon RD (1976) Acta Crystallogr Sect A 32:751
20. Zhang Q, Farrauto RJ (2011) Appl Catal A 395:64
21. Friedrich M, Teschner D, Knop-Gericke A, Armbrüster M (2012) J Catal 285:41
22. Lorenz H, Friedrich M, Armbrüster M, Klötzer B, Penner S (2013) J Catal 297:151
23. Iwasa N, Takezawa N (2003) Top Catal 22:215
24. Kuc J, Matam SK, Neumann M, Yoon S, Thiel P, Armbrüster M, Weidenkaff A (2015) Catal Today. doi:10.1016/j.cattod.2015.01.002
25. Ota A, Kunkes EL, Kasatkin I, Groppo E, Ferri D, Poceiro B, Navarro Yerga RM, Behrens M (2012) J Catal 293:27
26. Kuc J, Zhang Y, Erni R, Yoon S, Karvonen L, Weidenkaff A, Matam SK (2015) Phys Status Solidi RRL 9:282